Turkish Journal of Engineering
https://dergipark.org.tr/en/pub/tuje
e-ISSN 2587-1366

Single and multisite detailed kinetic models for the adsorption and desorption of NO_2 over Cu based NH_3-SCR catalyst

Selmi Erim Bozbağ[*1]

[1] *Koç University, College of Engineering, Department of Chemical and Biological Engineering, Sarıyer, Istanbul, Turkey*

Keywords
NO_2 storage
NH_3 storage
Kinetic model
TPD
NH_3-SCR

ABSTRACT

Kinetic modeling of NH_3 Selective Catalytic Reduction (NH_3-SCR) of NOx in Cu-chabazite washcoated monolithic reactors has recently become an important task for design, control and calibration of heavy-duty engine aftertreatment systems. Development of detailed and accurate kinetic models rely on the correct simulation of the NO_2 and NH_3 storage at different conditions. Here, different kinetic schemes for NO_2 adsorption and desorption were developed and compared to experimental data. For this purpose, firstly, realistic values of the active Cu sites in the Cu-zeolite were obtained using the temperature programmed desorption (TPD) of NH_3 and NO_2 which showed fractional coverages of 0.04 and 0.17 for the so-called ZCuOH and Z_2Cu species which reside in the 8 and 6 membered rings (MR) of the zeolitic framework, respectively. Active site concentrations were used in the kinetic models which included simultaneous formation of nitrate/nitrite species or the formation of HNO_3 intermediate which in turn resulted in the formation of nitrates or nitrites over the ZCuOH. Models also included or excluded the NO_2 storage over the so called secondary Z_2Cu sites. It was shown that models taking into account HNO_3 intermediate formation along with two NO_2 storage sites were better fits to the experimental data.

1. INTRODUCTION

Ammonia Selective Catalytic Reduction (NH_3-SCR) is a widely used technology in the aftertreatment systems (ATS) of the lean-burn diesel powered light or heavy-duty vehicles for the abatement of harmful and toxic oxides of nitrogen (NOx). NH_3-SCR reactors usually are monolithic reactors with microchannels wash coated with active catalyst materials where NOx originating from the engine and NH_3 fed using the thermolysis of urea solution sprayed to the reactor undergo SCR reactions. Cu exchanged zeolites especially Cu-chabazites including Cu-SSZ-13 are the catalyst of choice by many original equipment manufacturers (OEMs) for NH_3-SCR process due high deNOx performance in a wide range of temperature and good hydrothermal stability (Gao et al. 2013; Paolucci et al. 2016a).

Over the recent years, there have been significant developments in the kinetic modeling of NH_3-SCR processes for NOx abatement which are usually aimed to be used in the design, calibration and control of SCR units (Bozbag et al. 2020b; Chatterjee et al. 2005; Chatterjee et al. 2007; Daya et al. 2018; Daya et al. 2020a; Dhillon et al. 2019; Gao et al. 2021; Olsson et al. 2015; Selleri et al. 2019; Supriyanto et al. 2015; Usberti et al. 2020). Unlike many industrial reactors, the reactors in the aftertreatment system are continually exposed to highly transient conditions in many cases due to different road conditions, speed and torque generated by the engine. These conditions require the models to be predictive in a variety of conditions for the calibration and control of urea dosage and for the prediction of downstream NOx and NH_3 concentrations. Thus, the underlying SCR mechanisms should be well emulated by the models otherwise cumulative NOx emissions could not be well predicted (Bendrich et al. 2020). Both NO_2 and NH_3 could be stored in Cu-chabazite catalysts at greater quantities and the surface NH_3 and NO_2 related species are important contributors to the catalytic mechanism of NH_3-SCR of NOx according to many authors (Bendrich et al. 2018; Bozbag et al. 2018; Clark et al. 2020; Greenaway et al. 2020; Janssens et al. 2015; Paolucci et al. 2017). Therefore, realistic kinetic modeling of NO_2 and NH_3 adsorption and desorption is crucial to correctly

* **Corresponding Author**
*(sbozbag@ku.edu.tr) ORCID ID 0000-0003-4471-2301

Cite this article
Bozbağ S E (2022). Single and multisite detailed kinetic models for the adsorption and desorption of NO_2 over Cu based NH_3-SCR catalyst. Turkish Journal of Engineering, 6(3), 230-237

Research Article / DOI: 10.31127/tuje.931038
Received: 01/05/2021; Accepted: 07/09/2021

represent the NH_3-SCR mechanism in order to obtain highly accurate transient NH_3-SCR models. This requires a realistic insight to the concentrations of the active sites on the catalyst for the calculation of total species rates using the mean field approximation where active site concentration normalized rate constants are used (Bozbag et al. 2020a; Daya et al. 2020b). It has been shown that the combined analysis of NH_3-TPD and NO_2-TPD profiles of Cu-chabazites could be used to quantify the concentration of two different Cu species often encountered in Cu-chabazites which are usually referred to as ZCuOH and Z_2Cu which occupy the 8MR and 6MR in the zeolite framework, respectively (Marberger et al. 2018; Paolucci et al. 2016b). Us and others (Bozbag et al. 2020a; Leistner et al. 2017; Luo et al. 2016) had shown that the NH_3-TPD peaks with centers at around 320 and 450^{o}C could be associated with Cu species residing at 6MR and 8MR, respectively. Combined with the known NH_3/Cu stoichiometry (Luo et al. 2017), one can calculate the surface concentrations. According to (Villamaina et al. 2019), NO_2-TPD could be used to titrate the ZCuOH concentrations which could be used as a validation of the surface concentrations obtained from NH_3-TPD. Along this line, different NO_2 adsorption-desorption mechanisms were modeled in the literature (Bendrich et al. 2018; Colombo et al. 2012; Olsson et al. 2009). While some of the models take into account the HNO_3 intermediate formation reactions (Bendrich et al. 2018) some do not (Colombo et al. 2012; Olsson et al. 2009). Moreover, these different NO_2 adsorption-desorption kinetic schemes have not been compared over the same fresh Cu-chabazite catalyst. Therefore, implications of using these different chemical schemes are yet to be discovered. There is also no model in the literature which accounts for multisite adsorption and desorption of NO_2.

For the case of the adsorption of NH_3 over Cu-chabazite, it has recently been suggested that upon adsorption, some Cu species undergo NH_3 solvation within the zeolitic cage and these NH_3 solvated Cu species which are in dynamic mobility might play a role in the SCR mechanism (Paolucci et al. 2017) or may not (Daya et al. 2021). On the other hand, in the literature, the active site values associated with the NH_3 adsorption desorption models is usually done quite arbitrarily and do not generally reflect the true number of active sites associated with adsorption and therefore the rate parameters associated with adsorption are usually lumped parameters. Thus, there is no multi-site kinetic model in the literature where the active site values used in the NH_3 adsorption-desorption model were validated by the NO_2 adsorption-desorption experiments as well.

In this study, a relatively easy method to evaluate different Cu species in Cu-chabazites based on NO_2 and NH_3 adsorption/desorption experiments is proposed and used to develop multisite kinetic models for NH_3 and NO_2 adsorption and desorption. The performance of different kinetic schemes for simulating NO_2 adsorption and desorption were compared to the experimental data obtained using a commercial Cu-chabazite catalyst. The mechanistic implications of using different models were determined.

2. METHOD

2.1. Laboratory tests

The catalysts used in this study were a commercial Cu-chabazite based formulation washcoated to cordierite monolith (400 cpsi – 4 mils). A cylindrical core with a length of 2.2 cm and a diameter of 1.9 cm was used in the runs. The experiments were carried out in a synthetic gas bench (SGB) described in (Bozbag et al. 2020a and 2020b). In a typical run, ceramic fiber paper wrapped monolith was loaded in a quartz reactor and placed in an electric tubular furnace (Thermo Scientific Lindberg Blue M) equipped with a PID controller enabling the desired temperatures or ramps for the experiments. The temperature at reactor inlet was constantly monitored using a J-type thermocouple placed 0.5 cm upstream of the catalyst. NH_3 was purchased from Elite Gaz (10% in He balance), NO_2 was purchased from Hatgaz (10% in N_2 balance), CO_2 and N_2 (5.0) were purchased from Airliquide. All gases were connected to and were fed to the reactor using respective calibrated mass flow controllers (Brooks Instruments) and H_2O was delivered using a peristaltic pump (Gilson Minipuls 3). During the experiments, a general mixture which contained CO_2, H_2O and N_2 passed initially through to a pre-heater after which they were fed to the reactor. NO_2 and NH_3, on the other hand, were fed to general mixture stream just before the reactor using three-way valves connected to inlet via compression fittings to avoid undesired gas phase reactions. All lines before and after the reactor was heated to 190 ^{o}C. The species concentrations at the outlet of the reactor were continuously monitored using MKS Multigas 2030 FTIR spectrometer. The catalyst was pre-treated (i.e. degreened) at 550 ^{o}C in the presence of 5% H_2O, 8% O_2, in N_2 for 2h at 40000 h^{-1} (NTP). Subsequent to the experiments, the catalyst was exposed to a stream consisting of 8% O_2 in N_2 at 550 ^{o}C for 30 min to clean the surface of any N-containing residues. All experiments were carried out at with a space velocity of 40000 h^{-1} (NTP). All the gas grades used were 5.0 or above.

NO_2 adsorption/TPD experiment consists of the adsorption, isothermal desorption, and Temperature Program Desorption (TPD) parts. In a typical experiment, NO_2 was introduced to the reactor (500 ppm NO_2, 5% H_2O, 10% CO_2 in N_2 balance), which evidently resulted in an adsorption breakthrough curve. Once adsorption was completed NO_2 feed was cut off and isothermal desorption of weekly bound NO_2 started during which feed stream contained 5% H_2O, 10% CO_2 in N_2 balance. After desorption of weakly bound NO_2 was completed, temperature ramp was started with a rate of 10 ^{o}C/min during which feed stream contained 5% H_2O, 10% CO_2 in N_2 balance as well.. NH_3 adsorption/TPD experiment was carried out in a similar manner. Feed conditions, reactor outlet concentrations and reactor inlet temperatures monitored during each experiment were presented in Section 3. Peak deconvolution was carried out using Fityk version 1.3.1. Gaussian peaks were added manually and then optimized using Nelder-Mead Simplex method.

2.2. Modeling

2.2.1. The reactor model

Modeling was performed using GT-POWER, version 2019 (GT-SUITE Exhaust Aftertreatment Application Manual 2019) using the Fixed Mesh (1+1D) solver and the details were provided elsewhere (Bozbag et al. 2020a). Briefly, mass, energy and momentum balances for the gas and washcoat phases were solved for each contributing gaseous and surface species. Film model was used to incorporate external mass transfer and a washcoat diffusion model was used to consider the effects of internal mass transfer.

2.2.2. Kinetic model

Reaction mechanisms and rate expressions for NO_2 adsorption/desorption (Model A, B, C, D) and NH_3 adsorption/desorption are presented in Table 1. The Arrhenius equation was used in the model to account for the temperature dependency of the turnover rate constant, k_j:

$$k_j = A_j e^{\frac{-E_{A,j}}{RT}} \quad (1)$$

where A_j is the pre-exponential factor and $E_{A,j}$ is the activation energy in reaction j. A coverage dependent activation energy function was used to describe the desorption of NH_3 from Z_2Cu sites (Reaction 11b):

$$E_{A,j} = E_{A,j,0}(1-\alpha\theta_k) \quad (2)$$

In Model A, the NO_2 adsorption and desorption occurred over ZCuOH sites accounting the simultaneous formation of ZCuONO and $ZCuNO_3$ surface species (Reaction 1). Formation of NO upon NO_2 adsorption was modeled using Reaction 2. In Model B, the formation of HNO_3 intermediate was accounted and $ZCuNO_3$ formation is based on reaction of ZCuOH and formed HNO_3 (Reaction 6). Model C is similar to Model A except additional NO_2 storage in terms of surface nitrites and desorption reaction were used over Z_2Cu sites. Model D is similar to Model B except additional NO_2 storage in terms of surface nitrites and desorption reaction were used over Z_2Cu sites. Thermal decomposition of surface nitrates was accounted in all of the models (Reactions 3 and 8). NH_3 adsorption and desorption was modeled using the reactions in Table 1.

The pre-exponential factors and activation energy values of Models A-D were optimized using the experimental data via a Genetic Algorithm to minimize the following error function which is also used to compare model performances:

$$Error = \frac{\left(\sum_{t=0}^{D_{exp}}(y_{NO,meas}-y_{NO,pred})^2 + \sum_{t=0}^{D_{exp}}(y_{NO_2,meas}-y_{NO_2,pred})^2\right)\Delta t}{2D_{exp}} \quad (3)$$

Kinetic parameters for NH_3 adsorption/desorption model were also optimized using a similar function.

Table 1 Reactions and Rate Expressions Used in the Models

Reaction Number	Reaction & Rate Expression
Reactions related to NO_2 adsorption/desorption for Model A (Rxn. 1-3) and Model C (Rxn. 1-4))	
1	$2ZCuOH + 2NO_2 \leftrightarrow ZCuONO + ZCuNO_3 + H_2O$
	$r_{1f} = k_{1f} C_{NO_2}^2 \theta_{ZCuOH}^2$, $r_{1b} = k_{1b} \theta_{ZCuNO_3} \theta_{ZCuONO}$
2	$NO_2 + ZCuONO \leftrightarrow NO + ZCuNO_3$
	$r_{2f} = k_{2f} C_{NO_2} \theta_{ZCuONO}$, $r_{2b} = k_{2b} C_{NO} \theta_{ZCuNO_3}$
3	$ZCuNO_3 + 0.5H_2O \rightarrow NO_2 + 0.25O_2 + ZCuOH$
	$r_{3f} = k_{3f} \theta_{ZCuNO_3}$
4	$Z_2Cu + NO_2 \leftrightarrow Z_2CuONO$
	$r_{4f} = k_{4f} C_{NO_2} \theta_{Z_2Cu}$, $r_{4b} = k_{4b} \theta_{Z_2CuONO}$
Reactions related to NO_2 adsorption/desorption for Model B (Rxn. 5-8) and Model D (Rxn. 5-9)	
5	$ZCuOH + 2NO_2 \leftrightarrow ZCuONO + HNO_3$
	$r_{5f} = k_{5f} C_{NO_2}^2 \theta_{ZCuOH}$, $r_{5b} = k_{5b} C_{HNO_3} \theta_{ZCuONO}$
6	$ZCuOH + HNO_3 \leftrightarrow ZCuNO_3 + H_2O$
	$r_{6f} = k_{6f} C_{HNO_3} \theta_{ZCuOH}$, $r_{6b} = k_{6b} \theta_{ZCuNO_3}$
7	$NO_2 + ZCuONO \leftrightarrow NO + ZCuNO_3$
	$r_{6f} = k_{6f} C_{NO_2} \theta_{ZCuONO}$, $r_{6b} = k_{6b} C_{NO} \theta_{ZCuNO_3}$
8	$ZCuNO_3 + 0.5H_2O \rightarrow NO_2 + 0.25O_2 + ZCuOH$
	$r_{8f} = k_{8f} \theta_{ZCuNO_3}$
9	$Z_2Cu + NO_2 \leftrightarrow Z_2CuONO$
	$r_{9f} = k_{9f} C_{NO_2} \theta_{Z_2Cu}$, $r_{9b} = k_{9b} \theta_{Z_2CuONO}$
Reactions related to NH_3 adsorption/desorption	
10	$NH_3 + Z_2W \leftrightarrow Z_2WNH_3$
	$r_{10f} = k_{10f} C_{NH_3} \theta_{Z_2W}$, $r_{10b} = k_{10b} \theta_{Z_2WNH_3}$
11	$4NH_3 + Z_2Cu1 \leftrightarrow Z_2Cu1(NH_3)_4$
	$r_{11f} = k_{11f} C_{NH_3} \theta_{Z_2Cu1}$, $r_{11b} = k_{11b} \theta_{Z_2Cu1(NH_3)_4}$
12	$3NH_3 + ZCuOH \leftrightarrow ZCuOH(NH_3)_3$
	$r_{12f} = k_{12f} C_{NH_3} \theta_{ZCuOH}$, $r_{12b} = k_{12b} \theta_{ZCuOH(NH_3)_3}$
13	$NH_3 + ZB \leftrightarrow ZBNH_3$
	$r_{13f} = k_{13f} C_{NH_3} \theta_{ZB}$, $r_{13f} = k_{13b} \theta_{ZBNH_3}$

3. RESULTS AND DISCUSSION

Figure 1 displays the typical TPD of NH_3 (Fig. 3a) and TPD of NO_2 (Fig. 3b) over Cu-chabazite. The NH_3-TPD profile was fitted with 3 Gaussian peaks with peaks centers at 355, 474 and 534 ˚C which were ascribed to Z_2Cu, ZCuOH and Brönsted sites, respectively. Isothermal desorption of NH_3 observed upon the cutting off of the NH_3 feed was associated with species which bound to NH_3 weakly (hereafter referred to as Z_2W sites). Among these sites W and Cu were assumed to occupy two zeolitic sites whereas CuOH and B sites occupied a single zeolite site. The NH_3 storages associated with Z_2W, Z_2Cu, ZCuOH and Brönsted sites (ZB) were 119.1, 107.6, 34.2 and 9.7 mol/m^3. NO_2-TPD profile was fitted with two Gaussian peaks with peak centers at 302 and 365 ˚C and with NO_2 storage values of 5.9 and 12.3 mol/m^3, respectively. The peak at the 365 ˚C was assigned to NO_2 storage at ZCuOH species according to the literature (Villamaina et al. 2019) and the peak at the 302 ˚C was tentatively assigned to NO_2 storage on Z_2Cu species.

To develop a kinetic model based on realistic active site values, these storage values need to converted to active site concentration values via invoking a stoichiometric reaction between NH_3 or NO_2 and the active sites (Table 2). In the literature, it was shown that the ZCuOH sites could accommodate 3 NH_3 molecules, whereas the Z_2Cu sites could accommodate 4 (Villamaina et al. 2019). This stoichiometry was implemented in the kinetic model developed in this study. The measured NH_3 storage associated with the ZCuOH sites (34.2 mol/m^3) was in excellent agreement with the ZCuOH surface concentrations obtained using the NO_2-TPD which was 12.3 mol/m^3 which is approximately 3 times higher than the NH_3 storage measured for this site in line with the ZCuOH/NH_3 stoichiometry reported in the literature (Luo et al. 2017; Luo et al. 2016; Villamaina et al. 2019). Zeolitic site density occupied by each active site and corresponding fractional coverages were thus calculated based on the stoichiometries given in Table 1 and were presented in Table 2. For example, the fractional coverage of Z_2Cu sites in zeolite was calculated via dividing the NH_3 storage associated with this site by 4 (Reaction 11) followed by multiplication by 2 since 1 Cu site is occupied two zeolite sites. The fractional coverage values given in Table 2 were then used to develop the realistic active site based 4-site kinetic model of the adsorption and desorption of NH_3 over Cu-chabazite. From Table 2, it is clear that the NO_2 storage associated with Z_2Cu sites is low as compared to the fractional coverage of Z_2Cu sites obtained from NH_3-TPD, this indicated that only a small portion of the Z_2Cu sites could accommodate NO_2.

Table 2. Storage values and site density of the active sites

Sites	NO_2 stored[a]	NH_3 stored[a]	Site density[a]	Fractional coverage
Z_2W	0	119.1	238.1	0.76
Z_2Cu	5.9	107.6	53.7	0.17
ZCuOH	12.3	34.2	12.3	0.04
ZB	0	9.7	9.7	0.03

[a]: Units of mol/m^3

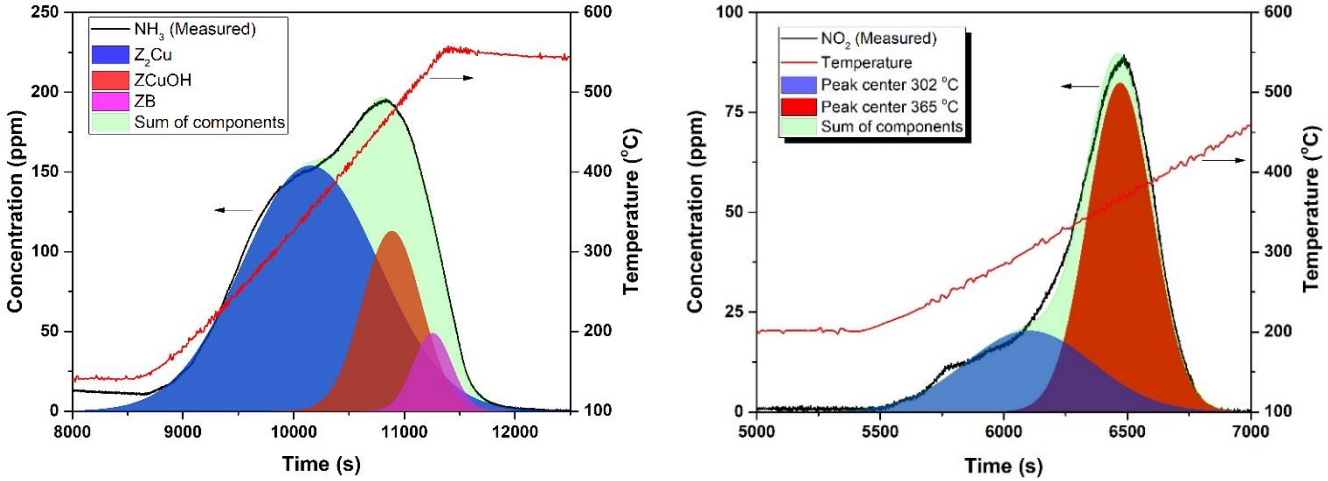

Figure 1. TPD profiles with deconvoluted components (a) NH_3, (b) NO_2.

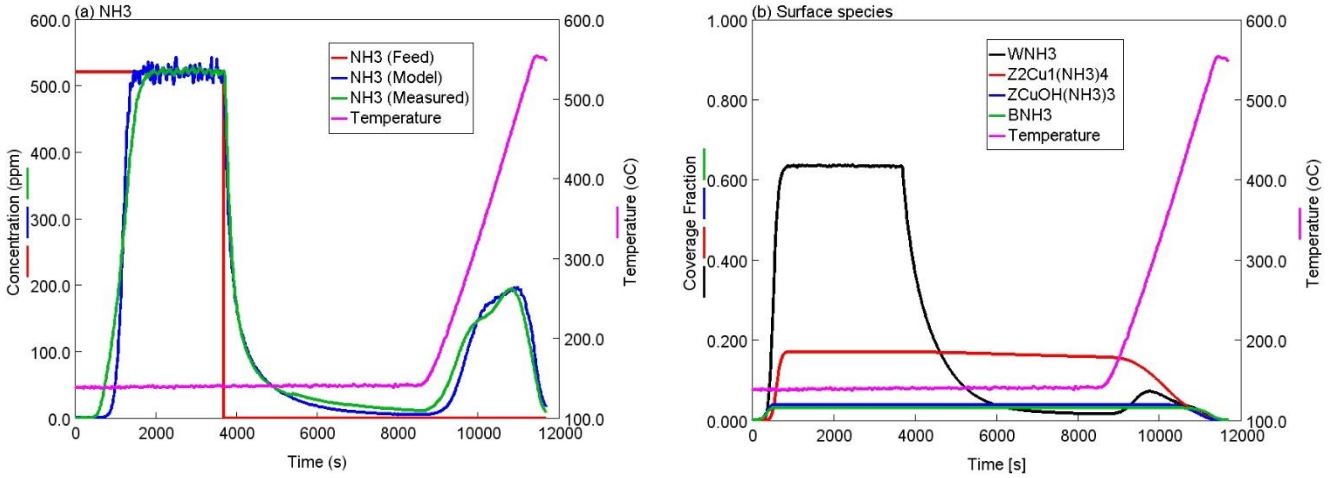

Figure 2. (a) Experimental and predicted NH_3 concentrations during NH_3 adsorption/TPD experiment (b) Simulated fractional coverages for the experiment given in (a).

Measured and modeled NH_3 outlet concentrations during NH_3 adsorption, isothermal desorption and TPD experiment are presented in Figure 2a. Here, upon delivery of the NH_3 feed at t=0 s to the reactor, the experimental data showed NH_3 breakthrough which succeeded the time lag period associated with NH_3 storage over the Cu-chabazite catalyst. Isothermal desorption of NH_3 was observed upon termination of the NH_3 feed at t=3699 s which was followed by the NH_3-TPD phase upon increase of the temperature. TPD profile manifested two main peaks with centers around 350 and 470 ˚C in agreement with previous reports (Leistner et al.

2017). Model (Table 1) showed excellent agreement with the measured data throughout the experiment including the adsorption breakthrough, isothermal desorption and TPD phases. The observed bimodal behavior of the TPD phase was well simulated and the relative intensities of the peaks were also well described by the model.

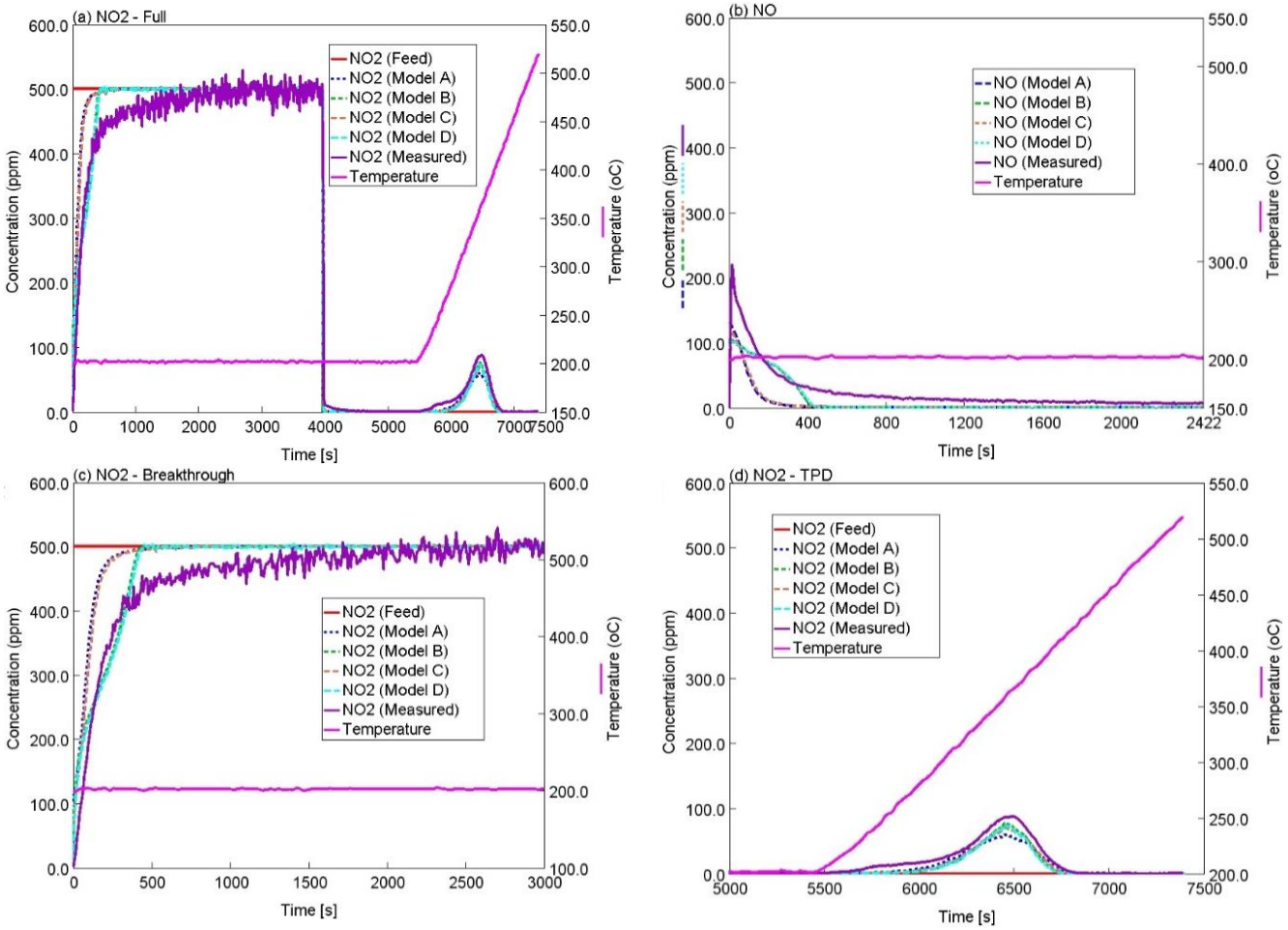

Figure 3. Experimental and predicted effluent concentrations during NO_2 adsorption/TPD experiment (a) NO_2, (b) NO, (c) NO_2 breakthrough region zoomed-up, (d) NO_2-TPD region zoomed-up.

Changes in the fractional coverages of the sites during the NH_3 adsorption and desorption calculated by the model were presented in Figure 2b. All of the NH_3 containing surface species converged to the initial fractional coverage of the corresponding active sites which showed the consistency of the model with measured site densities. Moreover, according to the kinetic model, the temperature centers of the desorption profiles of the $Z_2Cu(NH_3)_4$, $ZCuOH(NH_3)_3$ and $ZBNH_3$ species were in agreement with the deconvoluted temperature centers (355, 474 and 534 ˚C, respectively) associated with the sites containing the corresponding species obtained from the measured data demonstrating the realistic aspect of the developed kinetic model.

Adsorption and desorption behavior of NO_2 on Cu-chabazite along with its TPD profile is displayed in Figure 3a. NO_2 was fed to the reactor at t=0 which was followed by a slight lag time followed by an adsorption breakthrough which eventually reached the feed concentration which was 500 ppm. The observed lag time is associated with NO_2 stored in the catalyst mostly in terms of nitrates. NO_2 feed was stopped at t= 3969 s, which is followed by the rapid decrease of the NO_2 outlet concentrations as shown in Figure 3a. NO_2 release from the surface was observed in the TPD phase of the experiment. NO_2-TPD profile showed one main peak with temperature center of 363 ˚C and a shoulder at around 300 ˚C. The formation of NO is observed upon delivery of NO_2 as shown in Figure 3b. The formation of NO was ascribed to the reaction of NO_2 with ZCuOH sites as kinetically modeled using Reactions 2 and 7 depending on the models. Both NO_2 and NO outlet concentrations were well described by all of the models, however, some models were better than the others. NO_2 breakthrough region is enlarged in Figure 3c which showed Models B and D had better fits as compared to Models A and C. NO_2-TPD region is enlarged in Figure 3d which illustrated that Models B, C and D had similarly well fits to the experimental data whereas the Model A under-predicted NO_2 desorption. Quantitative description of model performances for simulating NO_2 and NO data during this experiment is illustrated in Figure 4 where the value of Eq. 3 for each model is shown. This revealed that the Model B captured the experimental data significantly better than Model A indicating the importance of HNO_3 modeling for NO_2 adsorption/desorption. Additionally, the utilization of second NO_2 storage site (Reactions 4 and 9 in Models C and D, respectively) decreased the

error of both Models A and B as shown with the decreased error values of Models C and D, respectively. This indicated that some of the NO_2 was indeed stored on a secondary storage site as this was hinted in NO_2-TPD curve (Fig. 1b) with a shoulder at around 300 ˚C. Although the storage capacity obtained from NO_2-TPD for Z_2Cu sites was low (which is in agreement with literature which showed that most of NO_2 was stored by the ZCuOH sites), Model C and D resulted in being better fits to experimental data than Models A and B, respectively, indicated that some NO_2 was in fact stored by the Z_2Cu sites at least to some extent. Better fits of Model C and D were due to the incorporation of Reactions 4 and 9 which accounted for additional NO_2 uptake over Cu-chabazite on the Z_2Cu sites.

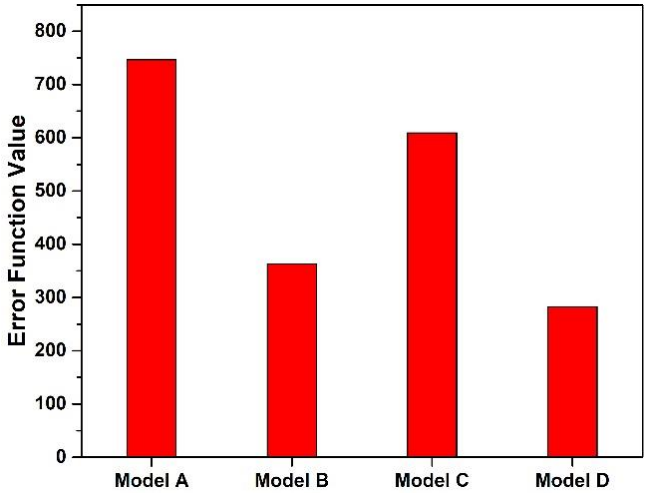

Figure 4. Error function values of different models investigated.

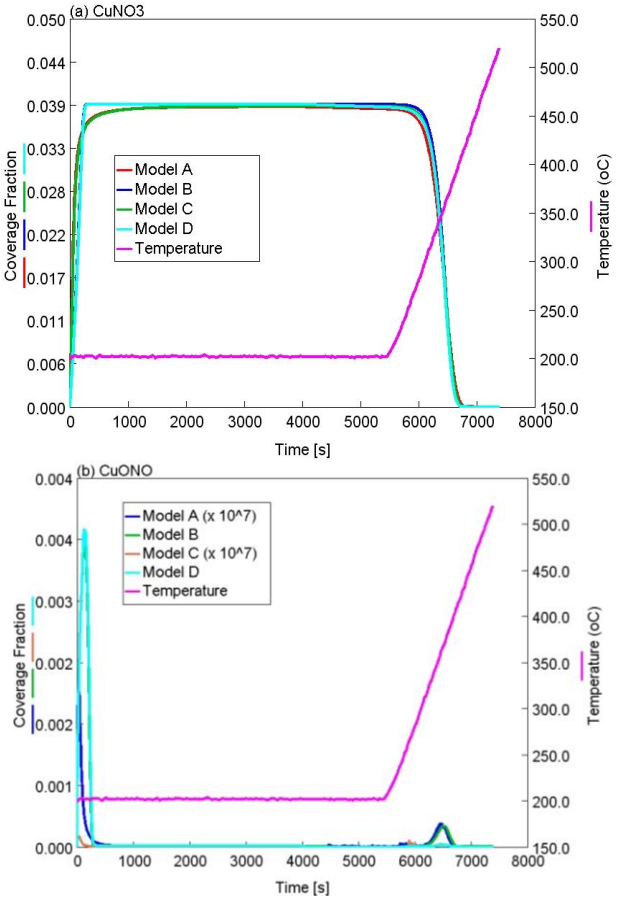

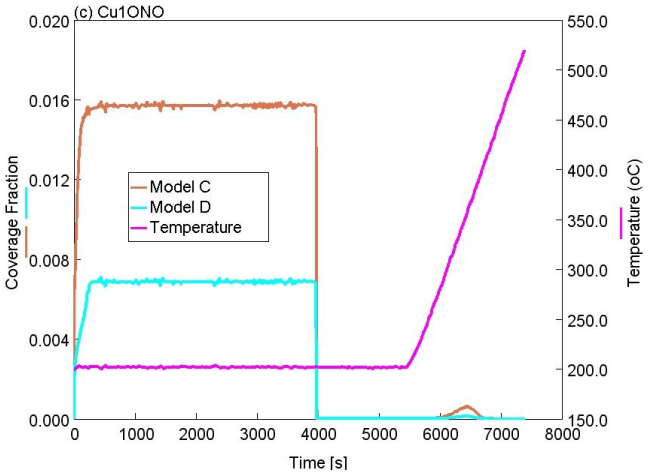

Figure 5. Simulated fractional coverages at the center of the reactor for (a) $ZCuNO_3$, (b) ZCuONO, (c) Z_2CuONO.

The fractional coverages of $ZCuNO_3$ (Figure 5a) and ZCuONO (Figure 5b) at the surface calculated at the center of the reactor showed that the nearly all of the Cu at the surface was in the form of $CuNO_3$ according to Models A and B as the fractional coverage of $ZCuNO_3$ while followed a similar trend to NO_2 breakthrough curve and finally reaching the fractional coverage value of 0.039 which was equal to the initial fractional coverage of ZCuOH. Fractional coverage of the $ZCuNO_3$ species dropped with increase in temperature during the TPD phase of the experiment due to the thermal decomposition (Reaction 3 and 8). Fractional coverage values of CuONO species shown in Figure 5b are very low and suggested that the CuONO species are fast transient intermediates. Calculated fractional coverages of Z_2CuONO are illustrated in Figure 5c which showed lower values as compared those of $ZCuNO_3$ species.

4. CONCLUSION

A method based on a combinatorial use of NH_3-TPD and NO_2-TPD data of Cu-chabazite is proposed to calculate the surface concentrations of ZCuOH and Z_2Cu species. NH_3-TPD calculated concentration of ZCuOH perfectly matched the one obtained from NO_2-TPD. Based on these values, a multisite NH_3 adsorption and desorption model was developed and it described the experimental data in a very successful manner. Moreover, four different NO_2 adsorption/desorption models were developed which included or excluded the HNO_3 intermediate formation and possibility of the NO_2 storage over ZCuOH and Z_2Cu sites. Based on the fits to the experimental data, Model B where HNO_3 intermediate formation is considered showed much lower error function values as compared to Model A where this reaction was not considered indicating a better representation of the experimental data by the Model B. The possibility of Z_2Cu sites for NO_2 storage was also investigated and the models which included the secondary NO_2 storage sites (Models C and D) showed lower error function values as compared to the ones who do not (Models A and B). This pointed out that the importance of modeling of both ZCuOH and Z_2Cu for NO_2 storage which should be taken into account to develop

accurate detailed transient kinetic models for NH_3-SCR over Cu-chabazites.

ACKNOWLEDGEMENT

Financial support from Ford Otomotiv San. A.Ş. is gratefully acknowledged.

Conflicts of interest

The authors declare no conflicts of interest.

NOMENCLATURE

A_j	Turnover pre-exponential constant for reaction *j*
C_i	Concentration of species *i* in the gas phase (mol/m^3)
D_{exp}	Simulation duration
$E_{A,j}$	Activation energy for reaction *j* ($kJ \times mol^{-1}$)
$E_{A,j,0}$	Activation energy for reaction *j* at zero coverage ($kJ \times mol^{-1}$)
k_j	Turnover rate constant for the reaction *j*
r_j	Reaction rate for reaction *j* ($mol \times s^{-1} \times mol_{site}^{-1}$)
$y_{i,meas}$	Measured molar fraction of species *i* (ppm)
$y_{i,pred}$	Predicted molar fraction of species *i* (ppm)

Greek letters

α	Coverage dependence factor
Δt	Time step
θ_k	Fractional coverage of species k

REFERENCES

Bendrich M, Scheuer A & Votsmeier M (2020). Importance of nitrates in Cu-SCR modelling: A validation study using different driving cycles. *Catalysis Today*. doi: https://doi.org/10.1016/j.cattod.2020.03.015

Bendrich V M, Scheuerb A, Hayesa R E & Votsmeierb M (2018). Unified mechanistic model for Standard SCR, Fast SCR, and NO2 SCR over a copper chabazite catalyst. *Applied Catalysis B: Environmental, 222* 76–87.

Bozbag S E, Şanlı D, Özener B, Hisar G & Erkey C (2020a). An Aging Model of NH3 Storage Sites for Predicting Kinetics of NH3 Adsorption, Desorption and Oxidation over Hydrothermally Aged Cu-Chabazite. *Catalysts, 10*, 411.

Bozbag S E, Şimşek M, Demir O, Şanlı D, Ozener B, Hisar G & Erkey C (2020b). Assessment of the Single-Site Kinetic Model for NH3-SCR on Cu-Chabazite for the Prediction of NOx Emissions in Dynamometer Tests. *Emission Control Science and Technology, 6*, 1.

Bozbag S E, Simsek M, Demir O, Sanli Yildiz D, Ozener H B., Hisar, G., & Erkey, C. (2018). Experimental and theoretical study of NH3 adsorption and desorption over a Cu-chabazite NH3-SCR catalyst. *Turkish Journal of Chemistry, 42*, 1768 – 1780.

Chatterjee D, Burkhardt T, Bandl-Konrad B, Braun T, Tronconi E, Nova I & Ciardelli C (2005). Numerical Simulation of Ammonia SCR-Catalytic Converters: Model Development and Application. *SAE Technical Paper Series, 2005-01-965*.

Chatterjee D, Burkhardt T, Weibel M, Nova I, Grossale A & Tronconi E (2007). Numerical Simulation of Zeolite- and V-Based SCR Catalytic Converters. *SAE Technical Paper Series, 2007-01-1136*.

Clark A H, Nuguid R J G, Steiger P, Marberger A, Petrov A W, Ferri D, . . . Kröcher O (2020). Selective Catalytic Reduction of NO with NH3 on Cu–SSZ-13: Deciphering the Low and High-temperature Rate-limiting Steps by Transient XAS Experiments. *Chemcatchem, 12*(5), 1429-1435. doi:10.1002/cctc.201901916

Colombo M, Nova I & Tronconi E (2012). Detailed kinetic modeling of the NH3-NO/NO2 SCR reactions over a commercial Cu-zeolite catalyst for Diesel exhausts after treatment. *Catalysis Today, 197*(1), 243-255. doi:10.1016/j.cattod.2012.09.002

Daya R, Desai C & Vernham B (2018). Development and Validation of a Two-Site Kinetic Model for NH3-SCR over Cu-SSZ-13—Part 2: Full-Scale Model Validation, ASC Model Development, and SCR-ASC Model Application. *Emission Control Science and Technology, 4*, 172–197.

Daya R, Joshi S Y, Dadi R K, Tang Y, Trandal D, Srinivasan A, . . . Cunningham M (2020a). An explicit reduced-order model of Cu-Zeolite SCR catalyst for embedding in ECM. *Chemical Engineering Journal*, 127473. doi: https://doi.org/10.1016/j.cej.2020.127473

Daya R, Joshi S Y, Luo J, Dadi R K, Currier N W & Yezerets A (2020b). On kinetic modeling of change in active sites upon hydrothermal aging of Cu-SSZ-13. *Applied Catalysis B: Environmental, 263*, 118368. doi: https://doi.org/10.1016/j.apcatb.2019.118368

Daya R, Keturakis C J, Trandal D, Kumar A, Joshi S Y & Yezerets A (2021). Alternate pathway for standard SCR on Cu-zeolites with gas-phase ammonia. *Reaction Chemistry & Engineering*. doi:10.1039/D1RE00041A

Dhillon P S, Harold M P, Wang D, Kumar A & Joshi S Y (2019). Modeling and analysis of transport and reaction in washcoated monoliths: Cu-SSZ-13 SCR and dual-layer Cu-SSZ-13 + Pt/Al2O3 ASC. *Reaction Chemistry & Engineering, 4*(6), 1103-1115. doi:10.1039/C8RE00325D

Gao F, Kwak J H, Szanyi J & Peden C H F (2013). Current Understanding of Cu-Exchanged Chabazite Molecular Sieves for Use as Commercial Diesel Engine DeNO(x) Catalysts. *Topics in Catalysis, 56*(15-17), 1441-1459. doi:10.1007/s11244-013-0145-8

Gao Z, Pihl J, LaClair T & Fricke B (2021). Global kinetic modeling of NH3-SCR with two sites of NH3 storage on Cu-SSZ-13. *Chemical Engineering Journal, 406*, 127120. doi: https://doi.org/10.1016/j.cej.2020.127120

Greenaway A G, Marberger A, Thetford A, Lezcano-González I, Agote-Arán M, Nachtegaal M, . . . Beale A M (2020). Detection of key transient Cu intermediates in SSZ-13 during NH3-SCR deNOx by modulation excitation IR spectroscopy. *Chemical Science, 11*(2), 447-455. doi:10.1039/C9SC04905C

GT-SUITE Exhaust Aftertreatment Application Manual. (2019). Gamma Technologies LLC.

Janssens T V W, Falsig H, Lundegaard L F, Vennestrom P N R, Rasmussen S B, Moses P G, . . . Beato P (2015). A Consistent Reaction Scheme for the Selective Catalytic Reduction of Nitrogen Oxides with Ammonia. *ACS Catalysis, 5*(5), 2832-2845. doi:10.1021/cs501673g

Leistner K, Xie K, Kumar A, Kamasamudram K & Olsson L (2017). Ammonia Desorption Peaks Can Be Assigned to Different Copper Sites in Cu/SSZ-13. *Catalysis Letters, 147*(8), 1882-1890. doi:10.1007/s10562-017-2083-8

Luo J, Gao F, Kamasamudram K, Currier N, Peden C H F & Yezerets A (2017). New insights into Cu/SSZ-13 SCR catalyst acidity. Part I: Nature of acidic sites probed by NH3 titration. *Journal of Catalysis, 348*, 291-299. doi: https://doi.org/10.1016/j.jcat.2017.02.025

Luo J, Wang D, Kumar A, Li J, Kamasamudram K, Currier N & Yezerets A (2016). Identification of two types of Cu sites in Cu/SSZ-13 and their unique responses to hydrothermal aging and sulfur poisoning. *Catalysis Today, 267*, 3-9. doi: https://doi.org/10.1016/j.cattod.2015.12.002

Marberger A, Petrov A W, Steiger P, Elsener M, Kröcher O, Nachtegaal M & Ferri D (2018). Time-resolved copper speciation during selective catalytic reduction of NO on Cu-SSZ-13. *Nature Catalysis, 1*(3), 221-227. doi:10.1038/s41929-018-0032-6

Olsson L, Sjovall H & Blint R J (2009). Detailed kinetic modeling of NOx adsorption and NO oxidation over Cu-ZSM-5. *Applied Catalysis B-Environmental, 87*(3-4), 200-210. doi:10.1016/j.apcatb.2008.09.007

Olsson L, Wijayanti K, Leistner K, Kumar A, Joshi S Y, Kamasamudram K, . . . Yezerets A (2015). A multi-site kinetic model for NH3-SCR over Cu/SSZ-13. *Applied Catalysis B-Environmental, 174*, 212-224. doi:10.1016/j.apcatb.2015.02.037

Paolucci C, Di Iorio J R, Ribeiro F H, Gounder R & Schneider W F (2016a). Chapter One - Catalysis Science of NOx Selective Catalytic Reduction With Ammonia Over Cu-SSZ-13 and Cu-SAPO-34. In C. Song (Ed.), *Advances in Catalysis* (Vol. 59, pp. 1-107): Academic Press.

Paolucci C, Khurana I, Parekh A A, Li S, Shih A J, Li H, . . . Gounder R (2017). Dynamic multinuclear sites formed by mobilized copper ions in NOx selective catalytic reduction. *Science, 357*(6354), 898-903. doi:10.1126/science.aan5630

Paolucci C, Parekh A A, Khurana I, Di Iorio J R, Li H, Albarracin Caballero J D, . . . Schneider W F (2016b). Catalysis in a Cage: Condition-Dependent Speciation and Dynamics of Exchanged Cu Cations in SSZ-13 Zeolites. *J. Am. Chem. Soc., 138*(18), 6028-6048. doi:10.1021/jacs.6b02651

Selleri T, Nova I & Tronconi E (2019). An efficient reduced model of NH3-SCR converters for mobile aftertreatment systems. *Chemical Engineering Journal, 377*, 120053. doi:https://doi.org/10.1016/j.cej.2018.09.214

Supriyanto Wijayanti K, Kumar A, Joshi S, Kamasamudram K, Currier N W, . . . Olsson L (2015). Global kinetic modeling of hydrothermal aging of NH3-SCR over Cu-zeolites. *Applied Catalysis B-Environmental, 163*, 382-392. doi:10.1016/j.apcatb.2014.07.059

Usberti N, Gramigni F, Nasello N D, Iacobone U, Selleri T, Hu W, . . . Tronconi E (2020). An experimental and modelling study of the reactivity of adsorbed NH3 in the low temperature NH3-SCR reduction half-cycle over a Cu-CHA catalyst. *Applied Catalysis B: Environmental, 279*, 119397. doi:https://doi.org/10.1016/j.apcatb.2020.119397

Villamaina R, Liu S, Nova I, Tronconi E, Ruggeri M P, Collier J, . . . Thompsett D (2019). Speciation of Cu Cations in Cu-CHA Catalysts for NH3-SCR: Effects of SiO2/AlO3 Ratio and Cu-Loading Investigated by Transient Response Methods. *ACS Catalysis, 9*(10), 8916-8927. doi:10.1021/acscatal.9b02578